Topography of the motion aftereffect with and without eye movements

Ali Ezzati

School of Cognitive Sciences,
Institute for Research in Fundamental Sciences (IPM),
Tehran, Iran, &
Research Center for Brain and Cognitive Sciences,
Shaheed Beheshti University of Medical Sciences,
Tehran, Iran

Ashkan Golzar

Department of Neurological and Vision Sciences,
University of Verona, Verona, Italy, &
School of Cognitive Sciences,
Institute for Studies in Theoretical Physics
and Mathematics, Tehran, Iran

Arash S. R. Afraz

Harvard University, Cambridge, MA, USA,
Institute for Studies in Theoretical Physics
and Mathematics, Tehran, &
Shaheed Beheshti University of Medical Sciences,
Tehran, Iran

Although a lot is known about various properties of the motion aftereffect (MAE), there is no systematic study of the topographic organization of MAE. In the current study, first we provided a topographic map of the MAE to investigate its spatial properties in detail. To provide a fine topographic map, we measured MAE with small test stimuli presented at different loci after adaptation to motion in a large region within the visual field. We found that strength of MAE is highest on the internal edge of the adapted area. Our results show a sharper aftereffect boundary for the shearing motion compared to compression and expansion boundaries. In the second experiment, using a similar paradigm, we investigated topographic deformation of the MAE area after a single saccadic eye movement. Surprisingly, we found that topographic map of MAE splits into two separate regions after the saccade: one corresponds to the retinal location of the adapted stimulus and the other matches the spatial location of the adapted region on the display screen. The effect was stronger at the retinotopic location. The third experiment is basically replication of the second experiment in a smaller zone that confirms the results of previous experiments in individual subjects. The eccentricity of spatiotopic area is different from retinotopic area in the second experiment; Experiment 3 controls the effect of eccentricity and confirms the major results of the second experiment.

Keywords: motion aftereffect, remote motion aftereffect, adaptation, retinotopic, spatiotopic, topography, eye movements

Citation: Ezzati, A., Golzar, A., & Afraz, A. S. R. (2008). Topography of the motion aftereffect with and without eye movements. *Journal of Vision, 8*(14):23, 1–16, http://journalofvision.org/8/14/23/, doi:10.1167/8.14.23.

Introduction

Motion aftereffect is one of the oldest reported visual phenomena (Verstraten, 1996). This effect has been studied extensively and there are several studies on temporal and spatial properties of MAE (Fang & He, 2004; Mareschal, Ashida, Bex, Nishida, & Verstraten, 1997; Mather, Verstraten, & Anstis, 1998; Pettigrew, Sanderson, & Levick, 1986). It is widely accepted that MAE is the result of neural adaptation of the direction-selective neurons in the visual system (Mather et al., 1998). Direction-selective neurons are found in multiple levels of primate visual system hierarchy; from subcortical structures to high-level cortical areas (Albright, 1984; De Valois, Yund, & Hepler, 1982; Geesaman, Born, Andersen, & Tootell, 1997; Grill-Spector & Malach, 2004; Tolias, Smirnakis, Augath, Trinath, & Logothetis, 2001). Therefore, the perceptual experience of MAE—most probably—results from neural adaptation in multiple layers of the visual hierarchy.

Almost all of the early and mid-level visual brain areas are topographically and retinotopically organized (Adams & Horton, 2003; Fize et al., 2003; Huk, Dougherty, & Heeger, 2002; Lyon et al., 2002; Palmer, 1999; Tootell et al., 1995). However, the resolution of space representation is highly various among these brain areas. Generally,

doi: 10.1167/8.14.23 Received August 18, 2007; published December 18, 2008 ISSN 1534-7362

lower cortical areas such as primary visual cortex represent visual space very accurately and neurons in these areas have very small receptive fields (Daniel & Whitteridge, 1961; Tootell, Hamilton, Silverman, & Switkes, 1988; Tootell, Silverman, Hamilton, De Valois, & Switkes, 1988; Tootell, Switkes, Silverman, & Hamilton, 1988). On the other hand, larger receptive fields of higher cortical areas correspond to less accurate but more global representation of the visual space (Albright & Desimone, 1987; Desimone & Ungerleider, 1986; Gattass & Gross, 1981; Gattass et al., 2005; Tootell et al., 1995; Van Essen, Maunsell, & Bixby, 1981). Various perceptual properties of the MAE (e.g., its spatial resolution) probably reflect the contribution of multiple levels of visual hierarchy in this phenomenon. Accurate measurement of these perceptual properties can help us bridge the gap between visual perception and neural activity at different stages of visual information processing.

Although there are many studies in the literature about spatial properties of MAE (Culham, Verstraten, Ashida, & Cavanagh, 2000; Snowden & Milne, 1996, 1997; von Grünau, 1986; von Grünau & Dubé, 1992; Wade, Spillmann, & Swanston, 1996; Weisstein, Harris, Berbaum, Tangney, & Williams, 1977), there is no systematic study on the topographic organization of the motion aftereffect. The main goal of this study is to provide a clear and fine topographic map of the motion aftereffect to investigate its spatial properties.

In the first experiment of the current study, following adaptation to coherent motion in a large field, a small moving test stimulus was presented to null the MAE. This small probe was presented at all different locations of the adapting motion frame and its background across numerous adaptation trials. This paradigm helped us measuring the strength of MAE in a fine spatial grain and providing its topographic map.

Another major question about motion perception in particular and vision in general is that how the visual system deals with frequent displacement of the retinal image due to eye movements (Husain & Jackson, 2001; Ross, Morrone, Goldberg, & Burr, 2001; Werner & Chalupa, 2004). We make saccadic eye movements 3–5 times a second (Burr, 2004; Palmer, 1999). This splits our visual input into a sequence of discrete images. How perception of the visual world remains continuous and stable across saccades?

Retinotopic representations provide useful information about the absolute position of objects relative to the retina, but they are not sufficient for extracting the spatial properties of the visual scene when the eyes move. To explain the stability of visual perception across eye movements, spatiotopic representations are proposed (Colby & Duhamel, 1996; Melcher, 2005; Melcher & Morrone, 2003; Merriam & Colby, 2005).

Recent evidences have shown that the visual system integrates motion signals from the same spatial locations that are separated in the retinotopic representation following eye movements (Melcher & Morrone, 2003). In addition, Afraz et al. non-published results (2004, "Spatial invariance of motion aftereffect across eye movements," *Perception, 33,* ECVP Abstract Supplement) showed that following a saccadic eye movement, duration of MAE is longer for the retinal location that corresponds to a spatial location where the adaptation signal was presented before the saccade. Furthermore, d'Avossa et al. (2007) showed that the BOLD response of human area MT is modulated by gaze direction, generating spatial selectivity based on the screen coordinates (rather than the retinal coordinates). Although these studies indicate mechanisms within the motion processing system that correct eye-movement-induced retinal displacements, we still do not know how these mechanisms work across the space. Does MAE region completely shift to the new retinal location that corresponds to the spatial location of the adapting stimulus? Or the MAE, after an eye movement, expresses a bimodal distribution over space, corresponding to both retinal and spatial locations? What are the topographical properties of the spatially corrected MAE, if it exists?

The second experiment of the current study is concerned with topographic properties of the MAE after an eye movement. The general design of this experiment is similar to the first experiment except that subjects were asked to make a saccade and re-fixate to a new target following adaptation to motion at a certain retinal location. Subsequently the MAE was measured for several points in the visual field to see if there are independent retinotopic and spatiotopic components in the MAE. Results of this experiment help us compare the topographic properties of the aftereffect in the retinotopic and spatiotopic regions.

The third experiment is basically designed to control some possible confounding factors of the first two experiments. Full field topographic maps of the first two experiments result from a huge number of data points pooled from all subjects. It was almost impossible to collect this huge number of trials for each individual subject separately. Pooling the data across all subjects can possibly conceal individual differences due to personal attentional strategies (Chaudhuri, 1990, p. 74, id.) and other individual perceptual differences. Here, in the light of the results of the first two experiments, we targeted a smaller zone spanning the area between the retinotopic center and the spatiotopic center. This targeting strategy decreased the number of required data points and enabled us to map the topographic pattern of the MAE in the critical zone for individual subjects separately.

In addition, the eccentricity of the spatiotopic area was bigger than the retinotopic area in the second experiment. This could possibly affect the results. Experiment 3 is designed in a way that both retinotopic and spatiotopic areas fall in the same eccentricity following the saccade. Finally, a difficult fixation task is added to this experiment to make sure that subjects keep their gaze fixated properly throughout the experimental trials.

Experiment 1: The basic topography of the motion aftereffect

Methods

Observers

Twelve subjects, aged between 19 and 24, with normal or corrected-to-normal vision participated in the experiment. Ten of them did not have prior knowledge about visual adaptation and were naive to the purpose of the experiment.

Apparatus

The stimulus sequence generation and experimental control were done by MATLAB Psychophysics Toolbox (Brainard, 1997; Pelli, 1997) on a 3-GHz Intel PC processor. Images were displayed on a 19-in. flat, CRT, RGB, LG color monitor (800 H × 600 V pixel resolution at a 100-Hz frame rate, $\gamma = 1.93$). Subjects viewed the display binocularly with their heads fixed on a chin and forehead rest in a dark room. The viewing distance was 47 cm so the screen subtended 41.8° × 32.2°.

Stimuli

The adaptation display contained a set of moving random dots embedded in a 13° × 13° imaginary frame on a background of stationary random dots (see Figure 1). Each dot was a black or white square 0.22° (4 × 4 pixels) in size. Random dots within the motion frame were moving *leftward* at a constant speed of 5.5 degree/second during the adaptation. A "wrap around procedure" was used to reposition dots reaching the left border of the adaptation area (the dots disappeared at the left border and simultaneously reappeared again in the same row at the right border of the adaptation area). The test probe was a small 2.63° × 2.63° patch of moving random dots (the same dots as the adapting stimulus) that followed the adapting stimulus immediately. The test patch was filtered by a Gaussian envelope ($\sigma = 0.549$ degree) so that the test patch faded in the background with no sharp edge. The test probe was presented at a random location in a 23.35° × 23.35° test area containing the adapting motion frame and its neighboring areas.

Procedure

Each subject performed four blocks of trials: two adapted and two non-adapted blocks. The block order was assigned randomly for each subject. The procedure was the same for all trials (Figure 1). In order to measure the strength of MAE, we used a neutral-test method (Mather et al., 1998). Initially, subjects fixated at a small fixation point, which was presented in the middle of the screen. Subjects had strict instructions to maintain their fixation during the trial.

The adapting stimulus was shown for 40 seconds before each block starts and then for 5 seconds before each trial. On each trial, the adaptation phase was followed by presentation of the test patch in a randomly selected grid

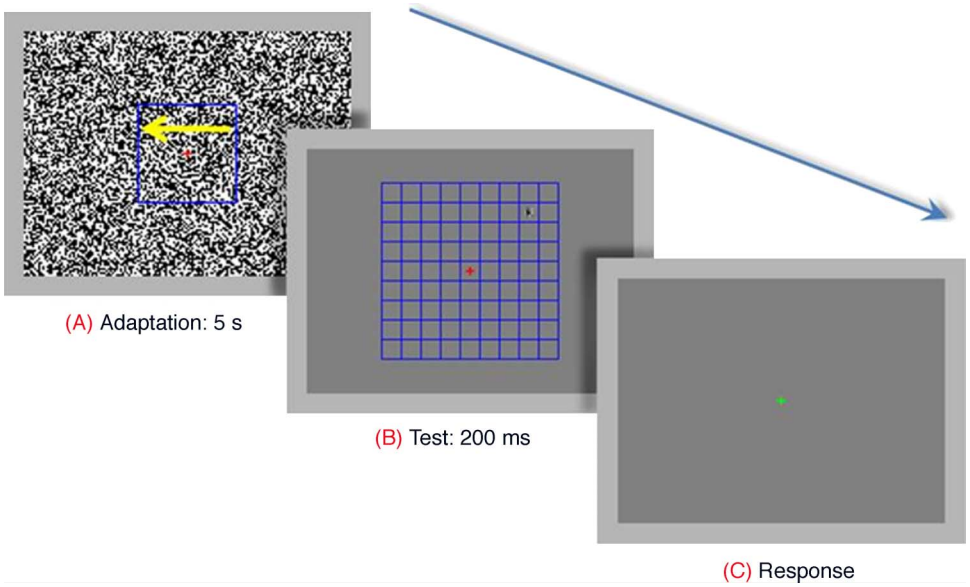

Figure 1. A trial of Experiment 1. (A) The adaptation stimulus was presented in the area inside the blue square for 5 seconds. (B) The test probe was displayed at a random location in the grid for 0.2 seconds, with a randomly chosen velocity. (C) Once the test stimulus disappeared, the color of the fixation point changed and the subject had to report the perceived motion direction of the test stimulus. Note that the blue square and the grid were not presented in the real task and are drawn merely for illustration purposes.

hole in a 9 × 9 grid spanning the 23.35° × 23.35° test area. The test duration was 200 ms. After the disappearance of the test pattern, the color of the fixation point changed from red to green and the subject had to press one of the two arrow keys on the keyboard to indicate the perceived direction of the test motion (rightward or leftward). The speed of random dots in the test patch was selected randomly among 11 possible values: 0, ±0.5, ±1, ±1.5, ±2, or ±3 degree/second, spanning subjects' psychophysical performance for motion direction discrimination (negative numbers account for leftward motion and positive numbers account for rightward motion). In each experimental block and in each grid hole, subjects were presented once with all 11 possible speeds. Each block contained 891 trials, and the total of 3564 trials were collected from each subject. The topographic map presented in Figure 3 is made based on 42768 trials collected from 12 subjects.

In non-adapted blocks, the same procedure was used, except that instead of the leftward motion signal during adaptation phase, we presented a set of moving non-correlated random dot pattern in the central 13° × 13° imaginary frame (the same as adapted blocks) on a background of stationary random dots. Non-adapted trials were used to provide a baseline for motion discrimination and to see if there is any asymmetry within the visual field for motion discrimination.

Data processing

The probability of reporting rightward motion for the test stimulus was plotted as a function of test stimulus speed (Figure 2). To determine the point of subjective equality (PSE), the psychometric function was approximated by fitting data to the following logistic function:

$$y = 1/(1 + \exp a(x + b)) \quad (1)$$

Positive values of b correspond to the leftward shift of the psychometric function. Motion aftereffect strength (MAS) was defined as the difference between the values of the parameter b for the adapted and non-adapted conditions. This difference (MAS) determines the PSE shift across conditions in the units of the abscissa (degree/second). MAS was determined for each of the grid holes independently.

Using binary logistic regression, we also used the Wald value as another measure of MAE magnitude. The Wald statistics is the ratio of square of the estimate of the regression coefficient (Bj) to the square of the estimate of its standard error (SE_{Bj}): Wald value = Bj^2/SE_{Bj}^2. The Wald value statistically determines the significance level of the adaptation effect. As expected, the Wald values and MAS values are highly correlated ($p < 0.001$, Spearman's ρ = 0.938). Analysis of the data based on Wald values instead of shift values (MAS) showed the same profile of results.

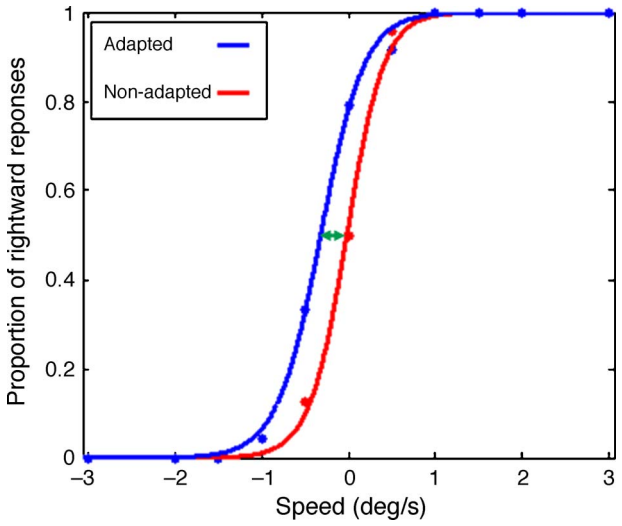

Figure 2. Psychometric function for the adapted and non-adapted conditions in one of the tested loci (indicated by ⋆ sign in the Figure 6). Adapting motion direction was always leftward. Positive and negative speed values in the abscissa indicate rightward and leftward motion directions of the test stimulus, respectively. The green arrow in this figure indicates the shift of the psychometric function due to adaptation (MAS value). The shift value in this example position is 0.16 degree/second ($p < 0.01$, binary logistic regression).

Results

For each test location, adaptation trials were pooled across all subjects (for more details, see Methods). The proportion of the "rightward motion" responses was plotted as a function of the test motion speed and MAS was measured for all test loci. (for more details, see Data processing section.)

Figure 3 illustrates the MAS values in the test grid holes. The middle 5 × 5 grid area corresponds to where the adapting motion signal had been presented before the test phase (adaptation frame). Grid holes containing significant psychometric shift (in terms of binary logistic regression, $p < 0.01$) are marked with green frames. Sharp boundaries of the MAE in this figure match perfectly with the adaptation frame (the middle 5 × 5 grid area in Figure 3). It also shows that the MAE is stronger on the internal edge of the adaptation area compared to its central parts. This "edge effect" is slightly stronger for the upper and lower edges (parallel to the motion direction) compared to the left and right edges (orthogonal to the motion direction). In order to examine spatial characteristics of MAE, we contrasted different regions of our map by grouping the data points of each region and performing binary logistic regression. Comparing the MAS inside and outside of the adaptation area (the middle 5 × 5 grid area in Figure 3) indicates that the MAE is expectedly more powerful in the area of adaptation ($p < 0.01$).

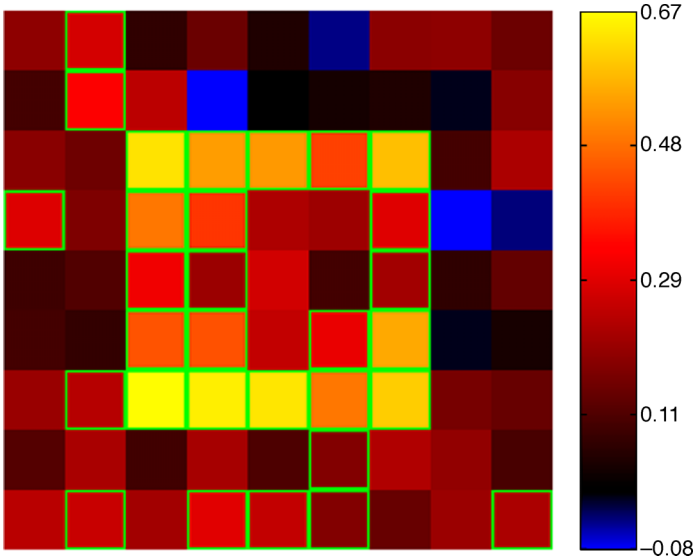

Figure 3. Topographic map of motion aftereffect. The color of each point in the map corresponds to the shift of the psychometric function at that point (PSE shift) following the adaptation. The fixation point was presented in the central grid hole. The adapting motion frame was presented in the central 5 × 5 grid of the map. Black corresponds to zero PSE shift; red/yellow and blue shades indicate positive (leftward) and negative (rightward) shift values, respectively. The vertical bar on the right shows the color map. The green frames indicate significant shift of the psychometric function for each grid hole.

In order to examine the possible higher strength of MAE on internal edges of the adaptation area (compared to the central part of the adaptation area and the background), we pooled the data in concentric square frames centered at the fixation point (see Figure 4A). Subsequently, the MAS value in each frame was measured (see Figure 4A). The results indicate that the MAS increases with respect to the size of the square frame inside the adaptation area; however, it drops abruptly outside the adaptation frame. The analysis also indicates that the MAS reaches its highest value at the inner edge of the adaptation area (Binary logistic regression, $p < 0.01$ in comparison with all other rectangular frames) (Figure 4B).

The MAS in bands parallel to the motion direction of the adapting stimulus was significantly ($p < 0.01$) higher than perpendicular bands in the internal edge of the adaptation area (Figure 4C).

Predomination of MAE in left VF ($p < 0.01$) was found both in the adaptation area and in the surrounding area. This is probably related to the leftward direction of the adapting motion.

Experiment 2: Topography of the motion aftereffect with eye movement

To measure the possibly independent components of the motion aftereffect, MAE was measured after an eye movement was made. Specifically, the subjects was instructed to make an eye movement after the adaptation and before the test phase to see if the MAE corresponds to the retinal location of the adapting stimulus or its spatial (screen) location.

Methods

Observers

Three subjects (two naive to the purpose of the experiment) with normal or corrected-to-normal vision

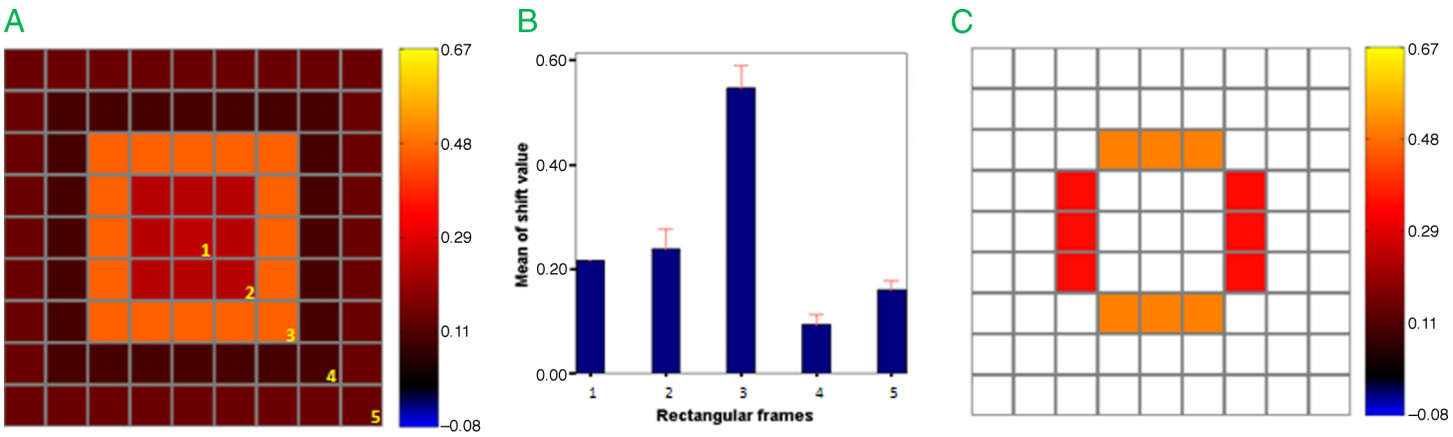

Figure 4. Planned contrast schema of the results of Experiment 1. (A) We compared the MAS in each of the concentric square frames with respect to the center. Color shades indicate the PSE shift value (MAS). The color code is the same as other figures. (B) MAS mean values in different concentric frames centered at the fixation point (center of the display). (C) Contrasting MAS in rectangular bands parallel to the direction of motion of the adapter with perpendicular bands shows that MAS is higher in the internal edges of the adapted region that are parallel to the direction of motion.

participated in this experiment. Subjects were all experienced psychophysics subjects.

Apparatus

The apparatus was the same as Experiment 1.

Stimuli

The stimuli were essentially the same as the previous experiment, only differing in the adapter size and the test area. The adapting motion region was a 10.5° × 10.5° square (approximately 16 times bigger than the size of the test probe) centered 6.5° below the center of the monitor screen (Figure 5A). The test probe was shown in the test area of 13° × 15.7° (5 × 6 grid holes) centered at the center of the screen (Figure 5C). In this configuration, the two top rows of the test area grid overlap with retinal adapted loci (referred to as the *retinotopic area*: marked with a purple frame in Figure 5C), whereas the two bottom rows overlap with the spatial location of the adapter on the display (referred to as the *spatiotopic area*: marked with a green frame in Figure 5C). To avoid collecting a huge number of trials by covering the whole field, retinotopic and spatiotopic sub-regions were sampled only from half of the original retinotopic and spatiotopic regions. The rest of the grid overlaps with neither retinal nor spatial loci. We referred to this area as the *non-adapted area* that contains the band between retinotopic and spatiotopic test areas, along with the leftmost and rightmost columns of the grid.

Procedure

Each subject performed 16 experimental blocks; eight adapted and eight non-adapted blocks. After adaptation phase (5 seconds), the fixation point disappeared and the subject was given an interval time of 500 ms to saccade to the newly presented fixation point, 13° above the initial location. Afterwards, the test stimulus was presented for 200 ms and the subject had to press one of the two arrow keys to indicate the perceived direction of motion (rightward or leftward; Figures 5A–5D).

All other procedural details were the same as Experiment 1.

Results

The MAS in each area was measured in the same way as the previous experiment. The topographic map can be partitioned into retinotopic, spatiotopic and non-adapted regions (Figure 5C). Each of the retinotopic and spatiotopic

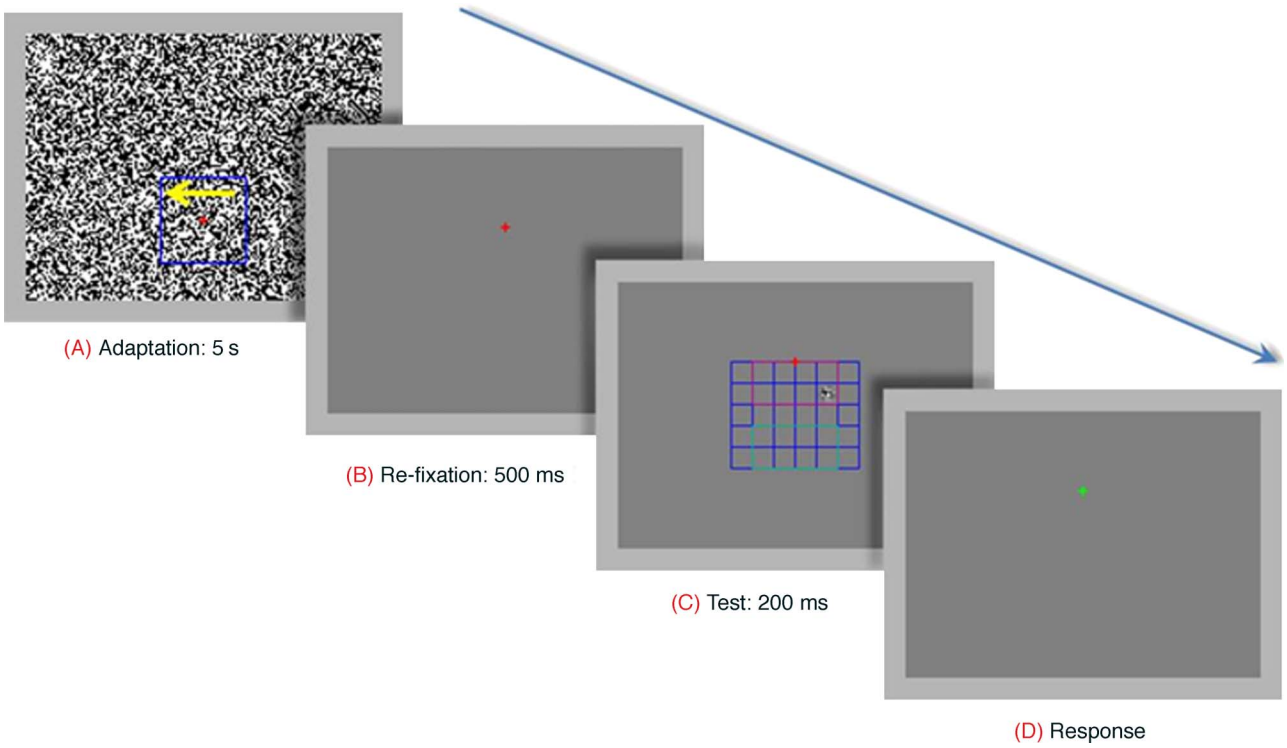

Figure 5. A trial of Experiment 2. (A) The adapting stimulus was presented in the area inside the blue square for 5 seconds. (B) The fixation point jumped to the new position. Subjects were given 500 ms to make a saccade and fixate on the new fixation point. (C) The test stimulus was randomly displayed in one of the 30 possible locations. The area inside the purple frame is part of the retinally adapted zone and the area inside the green frame is part of the spatially adapted zone. (D) Once the test stimulus disappeared and the fixation point color changed to green, the subject had to report the perceived direction of the test stimulus.

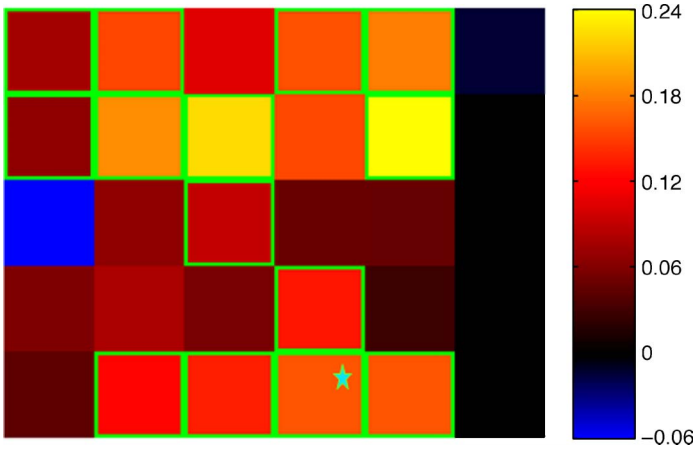

Figure 6. Topographic map of MAE after a saccade. Red/yellow and blue shades indicate positive and negative MAS values, respectively. Green frames highlight significant effects. The star (⋆) sign indicates the square for the psychometric function in Figure 2.

regions contains two primary bands. The lower band in the retinotopic area matches the edge of the adapter and here we call it *retinotopic-edge area*. The upper band in the retinotopic area matches the central band of the adapter and here we refer to it as *retinotopic-central area*. The upper band in the spatiotopic area corresponds to the adapter edges and we refer to it as *spatiotopic-edge area*. Finally, the lower band in spatiotopic area corresponds to the central part of the adapter and here we call it *spatiotopic-center area*. Figure 6 illustrates topographic map of the MAE after an eye movement. In order to examine the influence of the characteristics of these areas on the MAS, we carried out several pairwise planned contrasts in the three regions. We grouped together the data points of each region and performed binary logistic regressions.

We pooled the data in each of these four areas (retinotopic edge, retinotopic center, spatiotopic edge, and spatiotopic center; see Methods for details) and compared them to each other and also with the non-adapted area using binary logistic regressions (Figure 7A). The results show that

1. the MAS at the edge of the retinotopic area is significantly higher than the MAS of the non-adapted area ($p < 0.001$);
2. the MAS of the central retinotopic area is also higher than the MAS of the non-adapted area ($p < 0.01$);
3. the MAS of the edge of the retinotopic area is significantly higher than the MAS of the central retinotopic area ($p < 0.05$);
4. central spatiotopic area has a significantly bigger MAS than the non-adapted area ($p < 0.05$);
5. no significant difference is noticed between the edge of the spatiotopic area and the non-adapted area ($p = 0.10$); and finally
6. the MAS at the edge of the retinotopic area is significantly higher than the MAS of the central spatiotopic area ($p < 0.01$).

Figure 7B represents the mean of the MAS values in each horizontal band after discarding the rightmost and leftmost columns of the test area. According to the chart, the highest MAS values of all regions belong to retinotopic regions, followed by the spatiotopic areas (specially its central band).

The adapting stimulus used in the first two experiments was always presented moving leftward. This can cause a

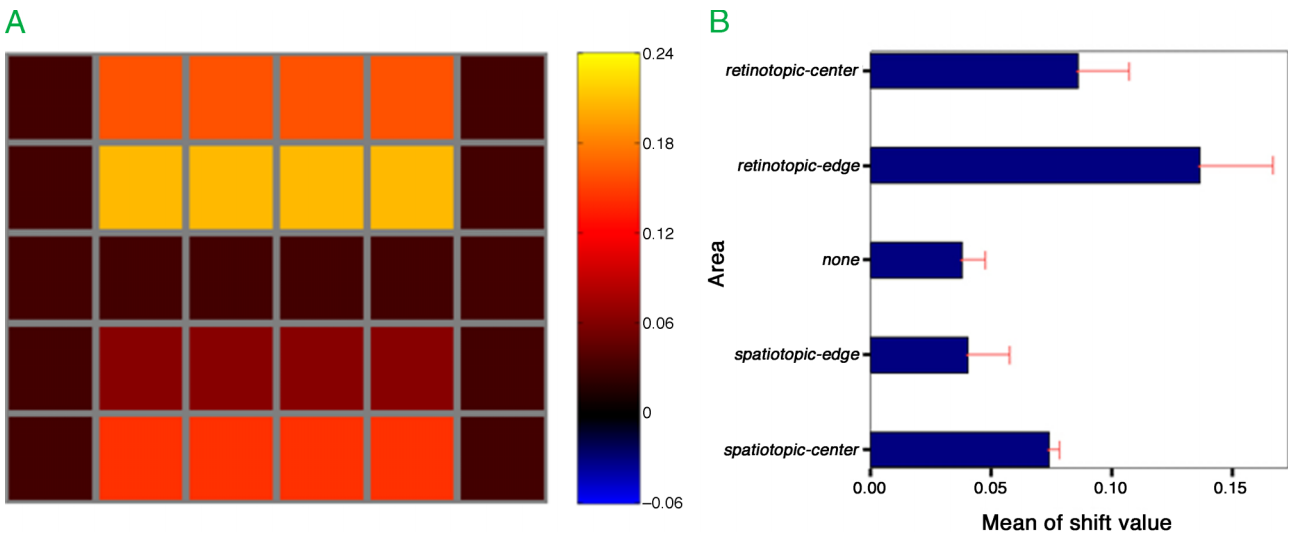

Figure 7. (A) Comparing different regions of the MAE topographic map after a saccade. Five different areas including retinotopic edge and central lines, spatiotopic edge and central lines, and the non-adapted area are contrasted based on their MAS values. (B) MAS mean values in different regions. In order to compare the critical areas of the map, the rightmost and leftmost columns of the test area were discarded and the mean value of MAS across each horizontal band was determined. The error bars represent one standard error of mean.

build-up of adaptation and possibly over-adapt the observer to leftward motion. Over-adaptation to leftward motion can shift the psychometric function too far in favor of the opposite direction and make the subjects identify even the strongest leftward motion signal as rightward. That would make the psychometric function flat and mess up the fitting and "PSE shift computation" procedure. This problem is fixed in our study by spanning a wide range of test motion signals. The two highest leftward motion speeds in our test were identified as leftward motion in all conditions. (The performance for identifying −3 and −2 degree/second speeds was >94% for all grid holes in the adapted condition.) This shows there was enough room for the PSE shift to avoid flattening of the psychometric curve and performance saturation. To investigate this possible problem more, we divided the data from each block of Experiment 2 into two chunks: first and second halves of each block. Comparing these two chunks of data can reveal possible confounding effects of adaptation build-up on the results. This new analysis showed very similar spatial pattern of MAE in both halves. The two patterns were highly correlated (Pearson's $r = 0.89$, $p < 0.01$).

Experiment 3

This experiment is basically a control experiment (see Introduction). In this experiment, adapter's position and saccade distance are designed in a way that both retinotopic and spatiotopic areas have the same distance from the fovea (see Figure 8 and compare it with Figure 5). In addition, to make sure that subjects kept their fixation properly through the trial, a difficult fixation task is added to the third experiment. Instead of the fixation task, eye movements were monitored through the experiment in one of the four subjects. The retinotopic and spatiotopic subregions are sampled only from one quarter of the original retinotopic and spatiotopic regions in a critical zone that spans retinotopic, non-adapted, and spatiotopic zones. This enabled us to collect sufficient data to provide topographic map of MAE separately for each subject.

Methods

Observers

Four subjects (two naive), aged between 22 and 24, with normal or corrected-to-normal vision participated in this experiment.

Apparatus

The apparatus was the same as previous experiments. For one of the subjects (subject AG), eye movements were recorded with a head-mounted video camera system for eye tracking (infrared video-based binocular eyetracking system Eyelink I, SMI; sampling rate 250 Hz), focused on

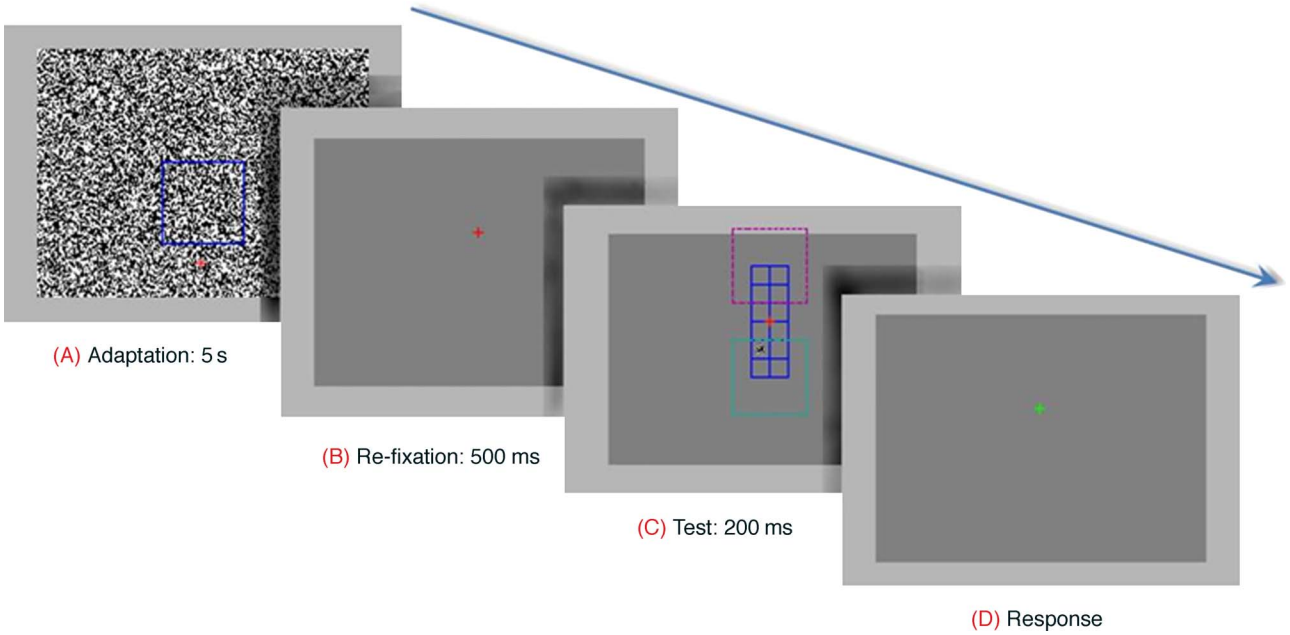

Figure 8. A trial of Experiment 3. (A) The adaptation stimulus was presented in the area inside the blue square for 5 seconds. (B) The fixation point jumped to a new position. Subjects were given 500 ms to make a saccade and fixate on the new fixation point. (C) The test stimulus was randomly displayed in one of the 12 possible test locations. The area inside the purple frame indicates the retinally adapted zone and the area inside the green frame represents spatially adapted zone. (D) Once the test stimulus disappeared and the fixation point color changed to green, the subject had to report the perceived direction of the test stimulus. If the fixation point dimmed during the trial, the subject had to press another key before reporting the perceived direction of the test stimulus.

both eyes of the subject. The spatial resolution of the system was <0.02 degree of visual angle. Online checking of saccade parameters was performed at each trial, and data were stored for offline analysis and in particular for detection and characterization of saccades and drifts. Trials began when the subject's gaze was within 1° distance from the center of the fixation point. Trials in which the subject's gaze drifted beyond this range during the presentation of the adapting stimulus or the test probe were discarded, and the same trials were repeated randomly along sessions. Overall, 6% of the total trials were thus repeated.

Stimuli

The stimuli were similar to previous experiments. In this experiment, the adapter frame size was the same as Experiment 2 (10.5° × 10.5°—approximately 16 times bigger than the size of test probe), centered 11.8° below the center of the screen (Figure 8A). Random dots within the motion frame were moving *leftward* in half of the adapted trials at a constant speed of 5.5 degree/second. In the rest of the adapted trials, the adapter had rightward direction with the same speed. The test probe was shown in the test area of 15.75° × 5.25° (6 × 2 grid wholes) centered at the center of the screen (Figure 8C). With this configuration, the two top rows of the test area grid overlap with retinally adapted zone (marked with a purple frame in the Figure 8C), whereas the two bottom rows overlap with the spatial location of the adapter on the display screen (marked with a green frame in Figure 8C). The rest of the test grid overlaps with neither retinal nor spatial loci (the two bands between retinotopic and spatiotopic test areas).

Fixation task: the luminance of a small hair cross (0.55° × 0.55°) within the fixation point was dimmed briefly (for 50 ms) very slightly (from 15.4 to 11.6 cd·m^{-2}). Subjects had to detect this small luminance change (see Procedure for more details).

Procedure

Each subject performed 48 experimental blocks: 24 adapted and 24 non-adapted blocks. Adapting motion direction was leftward in half of the adapted blocks; this direction was rightward for the rest of the blocks. After adaptation phase (5 seconds), the fixation point disappeared and the subject was given an interval time of 500 ms to saccade to the newly presented fixation point, 15.75° above the initial location. Afterwards, the test stimulus was presented for 200 ms in one of the twelve possible positions. The subject had to press one of the two arrow keys in order to indicate the perceived direction of the test motion (rightward or leftward; Figures 8A–8D). Other parameters were the same as previous experiments.

For three of the subjects (without eye monitoring), *fixation task* was presented alongside the main experiment. The fixation dimming occurred in 25% of trials, half of this happened during the adaptation period and the other half occurred during the test period. When detected the fixation point dimming, subjects had to press a key just before reporting the perceived direction of the test motion. The fixation task was extremely difficult and subjects had to maintain their fixation tightly to be able to perform the task above chance. In a separate test, we noticed that the performance in the fixation task (dimming detection) drops to chance level by fixating at a second fixation point only 1.3 degrees away from the original one.

Results

The MAS in each area was measured both for individual subjects and the data pooled from all subjects in the same way as the previous experiments. Figure 9 represents the map of the MAE for Experiment 3.

The map can be partitioned into retinotopic, spatiotopic, and non-adapted regions (Figure 8C). We grouped the data points of each region and performed binary logistic regressions (see Methods for details). Similar to experiment two, the top band in the retinotopic area represents *retinotopic-central area*. The bottom band in the retinotopic area stands for *retinotopic-edge area*. The top band in the spatiotopic area corresponds to *spatiotopic-edge area*. Finally, the bottom band in spatiotopic area corresponds to *spatiotopic-center area*. Pairwise planned contrasts in the different regions of the map were performed. The results show that

1. the MAS at the retinotopic area is significantly higher than the MAS of non-adapted area ($p < 0.001$ for all subjects);
2. the MAS of the spatiotopic area is also higher than the MAS of non-adapted area (AE, AG, FZ, $p < 0.05$—pooled data across subjects' $p < 0.05$);
3. the MAS in the retinotopic area was significantly higher than the spatiotopic area in two out of four subjects, the two other subjects showed higher MAS in retinotopic areas (comparing to the spatiotopic area) though it was not significant (pooled data across subjects' $p < 0.05$—AG, RN $p < 0.05$—AE $p = 0.24$—FZ $p = 0.12$);
4. no significant difference was noticed between the spatiotopic-edge area and the spatiotopic-center area ($p = 0.8$); and
5. no significant difference was observed between the retinotopic-edge area and the retinotopic-center area ($p = 0.1$).

This experiment also reveals some degree of individual differences in the spatial distribution of MAE. This differences might reflect minor differential anatomical and physiological constraints of the visual system and/or

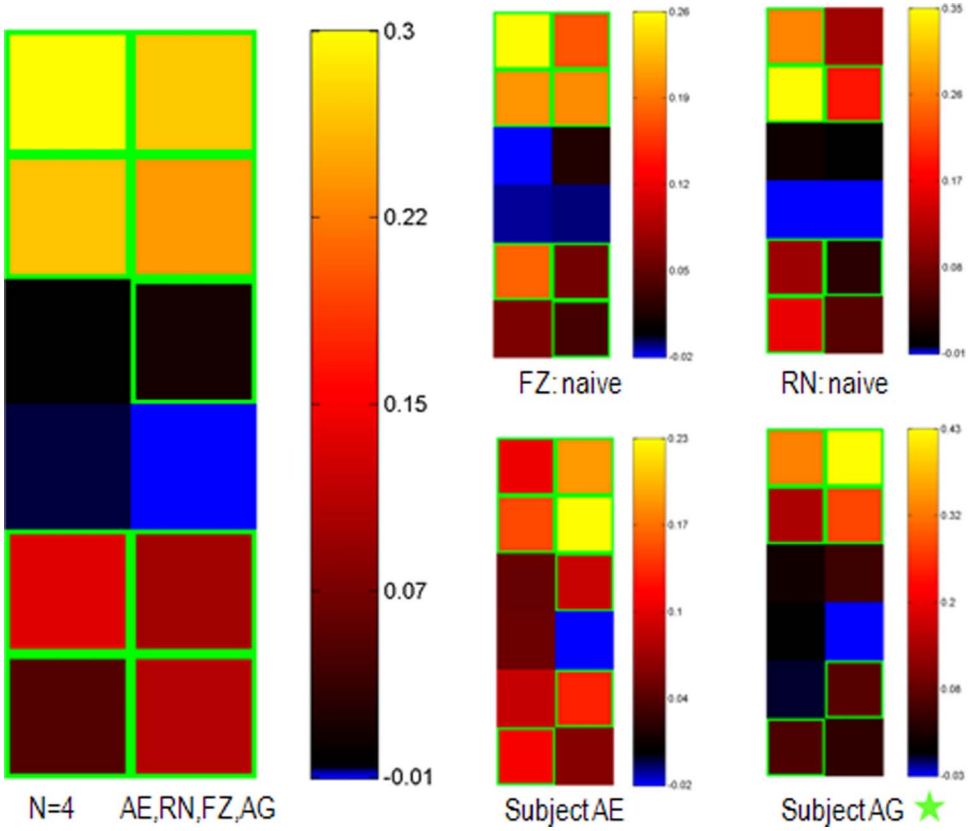

Figure 9. Topographic map of MAE after eye movement (Experiment 3). The big map on the left shows the pattern of MAE resulted from pooled data across four subjects. The four smaller maps show data from individual participants. The color maps are shown next to the figures. Like other color maps, positive and negative shift values are shown in red/yellow and blue shades, respectively. Green frames highlight significant shifts. For Subject AG (Marked by a green Star), eye movements were recorded with a head-mounted video camera system for eye tracking.

differential distribution of attention during the task, across the four tested subjects. It also might reflect the natural noise of the experimental paradigm. However, apart from minor individual differences, all subjects showed generally the same pattern of topographical findings. The average value of the MAS was biggest for the retinotopic area in all four subjects (0.21, 0.23, 0.17, and 0.30 in subjects FZ, RN, AE, and AG, respectively). This value was smaller for the spatiotopic area in all of the subjects (0.09, 0.09, 0.10, and 0.05, the same subject order) and smallest in the non-adapted band (−0.04, 0.01, 0.04, and 0.01, the same subject order) (please see Figure 9 for more details).

Figure 10A represents the map resulted from pooling the data of each of the horizontal bands. Figure 10B represents the mean of MAE shift values in each of the six bands. As the bar chart shows, the highest MAS values of all regions belong to retinotopic regions, followed by the spatiotopic areas.

For the *fixation tasks,* subjects successfully detected the luminance change in 90.5% (AE 90.6%, FZ 85.9%, RN 94.7%). One of the subjects performed the test, under eye tracking. The pattern of results obtained from this subject was the same as other subjects.

Discussion

The first experiment provides the topographic map of the motion aftereffect. One prominent effect in this map is the sharp transition between the adapted and non-adapted regions. This is consistent with previous studies, which revealed local properties of MAE (Anstis & Gregory, 1965). However, MAE can be translated across space even in areas that were not directly stimulated during the adaptation phase; this effect, named "remote motion aftereffect" (R-MAE), was reported first by von Grünau and Dubé (1992). We generally failed to get strong remote effects in this study and the boundary of the adapted region was very sharp. Remote motion aftereffect can be observed only when dynamical test patterns with bistable motion signals are used; this probably indicates different and possibly higher-level brain mechanisms underlying remote MAE (Mather et al., 1998). Sharp boundaries of the MAE region in our results suggest that neurons underlying static MAE have relatively small receptive fields (RFs) with well-defined borders. These neurons probably belong to lower-level brain areas in the visual hierarchy.

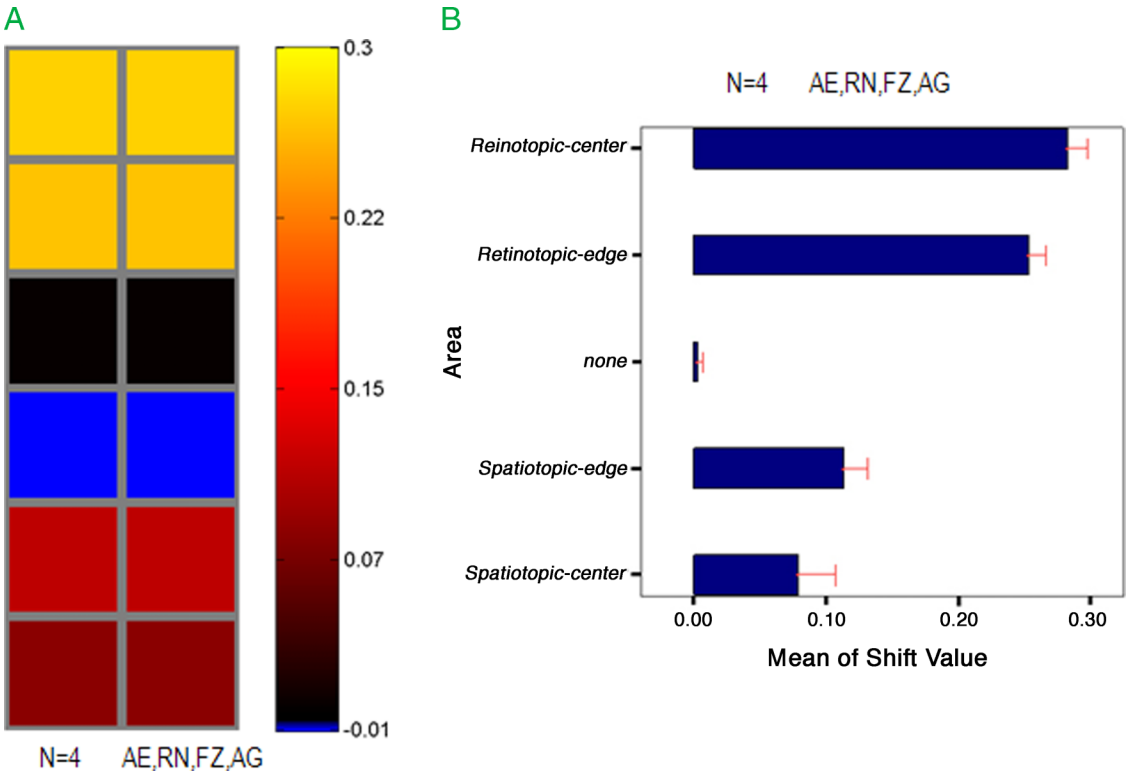

Figure 10. (A) Comparing different regions of the MAE map after the saccade. The horizontal bands are contrasted based on their MAS value. (B) MAS mean values in different regions. Bars show the mean value of MAS through six different areas including retinotopic edge and central bands, spatiotopic edge and central bands, and the non-adapted bands. The error bars represent one standard error of mean.

Several studies have shown the center-surround antagonistic nature of motion processing (Born, Groh, Zhao, & Lukasewycz, 2000; Born & Tootell, 1992; Eifuku & Wurtz, 1998; Jones, Grieve, Wang, & Sillito, 2001). Based on these findings, we expect neurons to respond more to motion signal on a static background than a large field motion signal. Tadin, Lappin, Gilroy, and Blake (2003) found that increasing the size of a high-contrast moving pattern renders its direction of motion more difficult to perceive and reduces its effectiveness as an adaptation stimulus. In addition, Reppas, Niyogi, Dale, Sereno, and Tootell (1997) reported robust fMRI activation in response to motion defined edges. Moreover, they showed this boundary-specific signal is present, and retinotopically organized, within early visual areas, beginning in the primary visual cortex (area V1). They also showed that motion boundary specific signal is largely absent from the motion-selective area MT/V5 and far extrastriate visual areas. These are consistent with our observation that MAE is stronger in the internal border of the motion area (compared to the central area). Considering presence of the motion boundary signal only in low-level visual areas, stronger MAE at internal edges of the adapted zone suggest involvement of low-level areas in this component of the motion aftereffect.

Consistently, Schatler and Zaidi (1993, p. 75, id.) showed that motion adaptation is smaller when the test stimulus is smaller than the adapting stimulus. Based on measurements of motion detection contrast elevation following adaptation to moving vertical gratings with different sizes (relative to the test stimulus), they built a model of motion adaptation that invokes diffuse inhibitory connections among motion-sensing mechanisms. Based on this model, central parts of a motion field receive bigger inhibition from neighboring motion detectors compared to the border area. This model implies weaker MAE in the central parts of the adapted region (due to receiving bigger inhibition during the adaptation) in contrast to the motion boundaries. The fact that MAE is weaker in the center of the adapted zone compared to the boundary of the motion area supports Sachtler and Zaidi's model for motion adaptation.

The motion on the horizontal edges of the adaptation square is "shearing motion" while the vertical contours of the adaptation square form "compression motion" (left side) and "expansion motion" (right side). Our results show sharper aftereffect boundary for the shearing motion compared to compression and expansion motion boundaries. At first glance, this suggests that motion spatial integration is larger in a direction parallel to the direction of motion. This is compatible to elliptical receptive fields, which their axis of elongation tends to be parallel to the preferred direction of motion, although, this view is not supported by physiological findings (Fredericksen,

Verstraten, & van de Grind, 1997; Raiguel et al., 1997; Raiguel, Van Hulle, Xiao, Marcar, & Orban, 1995; Xiao, Raiguel, Marcar, Koenderink, & Orban, 1995; Xiao, Raiguel, Marcar, & Orban, 1997). Consistent to our observation, van Doorn and Koenderink (1982) measured signal to noise ratios for coherently moving random dots embedded in random noise and found that transverse motion has lower threshold than compression motion. However, Nakayama, Silverman, MacLeod, and Mulligan (1985), using a different technique for measuring sensitivity, found the opposite result. In sum, regarding the background literature, it is hard to find a clear explanation for the observed difference between horizontal and vertical edges of the aftereffect zone. A contributory factor could be small tracking eye movements that smear the adaptation out of the adapting square at vertical edges.

The second experiment was designed to investigate how topography of the motion aftereffect changes after a saccadic eye movement. Eye movements change the image location on the retina, which consequently displaces the image on all retinotopic cortical areas including the primary visual cortex. Results of the first experiment showed strong topography for the motion aftereffect, this means that adapted neurons have accurate "spatial labels" and their imbalanced activity (due to adaptation) is perceived on their corresponding locations (probably their small receptive fields) across the visual field. The question arising here is what happens to these "spatial labels" after an eye movement? Are these spatial labels, or say, receptive fields (with the assumption that motion aftereffect is perceived at the RFs of adapted direction-selective cells) bound to their retinal location across eye movements, or are there mechanisms to correct space representation and spatial labeling of the adapted motion-selective neurons after the eye movement?

There are several lines of evidence in the literature that show both perceptual (Burr, 2004; Burr & Morrone, 2005; Melcher, 2005) and physiological (Berman, Heiser, Dunn, Saunders, & Colby, 2007; Berman, Heiser, Saunders, & Colby, 2005; Merriam & Colby, 2005; Merriam, Genovese, & Colby, 2003, 2007; Nakamura & Colby, 2002) updating of space representation in the visual field. In addition, it has been shown that motion signals can be temporally integrated over retinotopically different but spatially same loci across a saccade (Melcher & Morrone, 2003). There is also unpublished evidence which shows that after a saccade, remote motion aftereffect is stronger for new retinal location that corresponds to the spatial location of the adapting stimulus (Afraz et al., 2004, "Spatial invariance of motion aftereffect across eye movements," *Perception, 33,* ECVP Abstract Supplement). On the other hand, based on a long history of physiology and neuroimaging findings, it is evident that at least low-level brain areas with high-resolution topography (that are necessary to explain results of Experiment 1) are retinotopic (Adams & Horton, 2003; Tootell, Hamilton, et al., 1988; Tootell, Silverman, et al., 1988; Tootell, Switkes, et al., 1988) and we do not expect spatial updating across eye movements in these areas.

Results of Experiment 2 show that after an eye movement, the aftereffect map "splits" into separate retinotopic and spatiotopic regions. Figure 7B summarizes this effect; MAE is strongest at retinotopic and spatiotopic zones. This figure also shows that motion aftereffect is minimal in the band between retinotopic and spatiotopic zones (also see Figure 10 and results of Experiment 3). This narrow zone has a particular theoretical importance. One could possibly claim that the MAE observed in the spatiotopic location is the tail of a tapering gradient of MAE centered at the retinotopic locus and has nothing with spatiotopic representation. However, in that case, we cannot expect the dip in MAE in the narrow band between spatiotopic and retinotopic regions. The lack of the MAE in the band between the two zones is observed in both Experiments 2 and 3. In addition we did not see strong remote effects in Experiment 1. These observations make it difficult to consider the observed MAE in the spatiotopic zone as non-specific remote MAE.

Under usual experimental preparations with MAE, the two retinotopic and spatiotopic components of the MAE overlap, thus they are not separable. However, making a saccade between adaptation and test phases gives the experimenter the chance to separate these two components topographically. Existence of these two separate aftereffect zones probably indicates engagement of various levels of visual hierarchy in the MAE. Lower-level neural structures like V1 area are probably responsible for the retinotopic component of the MAE. This is the strongest component of the MAE. The "edge effect" observed in the retinotopic component of the aftereffect might be the signature of these low-level neural structures. As Figures 7A and 10 depict, the MAE is more pronounced on the internal edge of the retinotopic motion area (just like Experiment 1 results). On the other hand, in the spatiotopic region of the aftereffect, there is no such edge effect and the aftereffect in the middle of the spatiotopic zone is equally strong or even stronger than the edge (in case of Figure 7; Experiment 2 results). This perhaps indicates lower spatial resolution of neurons responsible for this component of the aftereffect and suggests higher-level origins of this component. These higher-level neurons are not affected that much by the motion energy near the local edges of the stimulus; instead, they code the global motion direction of the stimulus patch. Neurons with such RF properties can be found in extrastriate areas in the primate visual system, specifically in areas MT and MST (Albright, 1984; Maunsell & Newsome, 1987; Maunsell & Van Essen, 1983; Tanaka et al., 1986). Results of Reppas et al. (1997) suggest that motion-selective area MT and far extrastriate visual areas are possibly responsible for this spatiotopic component as boundary-specific signal is largely absent at these areas. In addition, a recent paper by d'Avossa et al. (2007) suggests spatiotopic representation of visual motion in human area

MT across saccadic eye movements. However, there are reports that failed to replicate this finding in human MT (Gardner, Merriam, Movshon, & Heeger, 2008; Vaziri et al., SFN 2007 Abstract).

Results of Experiment 3 confirm original findings of the first two experiments in individual subjects (please also see the Introduction). There was no fixation task in the first two experiments. One might claim that fixation drifts can bias the observed results. However, we expect any systematic fixation drift (at least drift toward the test stimulus which is the most likely fixation error) to smear out the MAE map and lead to uniform MAE across the space, which is clearly not the case in these results. Furthermore, replication of basic findings of the first two experiments in Experiment 3 in the presence of a difficult fixation task (in addition to eye tracking in one of the subjects of this experiment) rules out the possible effect of fixation errors as a major confounding factor.

The internal edge effect, observed in the results of the first two experiments is not replicated in Experiment 3. Several factors might be responsible for this. Most notably is the fact that the adapting motion was presented more peripherally in Experiment 3 compared to the first two experiments. Visual spatial resolution decreases drastically as the eccentricity increases; congruously, lateral interactions of motion detectors during the adaptation phase might work on a coarser spatial grain at larger eccentricities. As we only measured the MAE in a narrow band of the retinotopically corresponding zone, we might have missed the larger scale edge–center interactions within the adapted area. Alternatively, the lack of the internal edge effect in Experiment 3 might be attributed to the degraded spatial discrimination of the perceived aftereffect in the "test phase." According to this view, the internal edge effect fades at larger eccentricity because the observer cannot resolve the differential MAEs of the internal edge and the more central region at that eccentricity. This latter view, if true, casts shadow on some of our previous interpretations of the results of experiment two. There, the lack of internal edge effect in the spatiotopically corresponding zone was interpreted as the lack of the "signature" of low-level motion processing neural structures. In general, Experiment 3 opens the door for new questions about the internal edge effect: Does it scale with eccentricity? Does it correspond directly with visual discriminability of the MAE? Further studies, focused on this interesting topographic property of the MAE are required to nail down such questions and assumptions.

In summary, our findings provide methods for separating spatiotopic and retinotopic components of the MAE. The difference in the pattern of observed results for these two aftereffect zones suggests different levels of their underlying neural structures in the visual hierarchy. Further neuroimaging and physiology studies are needed to reveal neural basis of these separate components of the MAE more clearly.

Acknowledgments

We wish to thank Leonardo Chelazzi and Kourosh Mirpour for their helpful advice and Behrad Noudoost for his helpful comments throughout designing the experiments.

Commercial relationships: none.
Corresponding author: Ali Ezzati.
Email: ezzati@ipm.ir.
Address: School of Cognitive Sciences, Institute for Research in Fundamental Sciences (IPM), P.O. Box 19395-5746, Tehran, Iran.

References

Adams, D. L., & Horton, J. C. (2003). A precise retinotopic map of primate striate cortex generated from the representation of angioscotomas. *Journal of Neuroscience, 23,* 3771–3789. [PubMed] [Article]

Albright, T. D. (1984). Direction and orientation selectivity of neurons in visual area MT of the macaque. *Journal of Neurophysiology, 52,* 1106–1130. [PubMed]

Albright, T. D., & Desimone, R. (1987). Local precision of visuotopic organization in the middle temporal area (MT) of the macaque. *Experimental Brain Research, 65,* 582–592. [PubMed]

Anstis, S. M., & Gregory, R. L. (1965). The after-effect of seen motion: The role of retinal stimulation and of eye movements. *Quarterly Journal of Experimental Psychology,* 173–174.

Berman, R. A., Heiser, L. M., Dunn, C. A., Saunders, R. C., & Colby, C. L. (2007). Dynamic circuitry for updating spatial representations: III. From neurons to behavior. *Journal of Neurophysiology, 98,* 105–121. [PubMed] [Article]

Berman, R. A., Heiser, L. M., Saunders, R. C., & Colby, C. L. (2005). Dynamic circuitry for updating spatial representations. I. Behavioral evidence for interhemispheric transfer in the split-brain macaque. *Journal of Neurophysiology, 94,* 3228–3248. [PubMed] [Article]

Born, R. T., Groh, J. M., Zhao, R., & Lukasewycz, S. J. (2000). Segregation of object and background motion in visual area MT: Effects of microstimulation on eye movements. *Neuron, 26,* 725–734. [PubMed] [Article]

Born, R. T., & Tootell, R. B. (1992). Segregation of global and local motion processing in primate middle temporal visual area. *Nature, 357,* 497–499. [PubMed]

Brainard, D. H. (1997). The Psychophysics Toolbox. *Spatial Vision, 10,* 433–436. [PubMed]

Burr, D. (2004). Eye movements: Keeping vision stable. *Current Biology, 14,* R195–R197. [PubMed] [Article]

Burr, D., & Morrone, M. C. (2005). Eye movements: Building a stable world from glance to glance. *Current Biology, 15,* R839–R840. [PubMed] [Article]

Chaudhuri, A. (1990). Modulation of the motion aftereffect by selective attention. *Nature, 344,* 60–62. [PubMed]

Colby, C. L., & Duhamel, J. R. (1996). Spatial representations for action in parietal cortex. *Cognitive Brain Research, 5,* 105–115. [PubMed]

Culham, J. C., Verstraten, F. A., Ashida, H., & Cavanagh, P. (2000). Independent aftereffects of attention and motion. *Neuron, 28,* 607–615. [PubMed] [Article]

Daniel, P. M., & Whitteridge, D. (1961). The representation of the visual field on the cerebral cortex in monkeys. *The Journal of Physiology, 159,* 203–221. [PubMed] [Article]

d'Avossa, G., Tosetti, M., Crespi, S., Biagi, L., Burr, D. C., & Morrone, M. C. (2007). Spatiotopic selectivity of BOLD responses to visual motion in human area MT. *Nature Neuroscience, 10,* 249–255. [PubMed]

Desimone, R., & Ungerleider, L. G. (1986). Multiple visual areas in the caudal superior temporal sulcus of the macaque. *Journal of Comparative Neurology, 248,* 164–189. [PubMed]

De Valois, R. L., Yund, E. W., & Hepler, N. (1982). The orientation and direction selectivity of cells in macaque visual cortex. *Vision Research, 22,* 531–544. [PubMed]

Eifuku, S., & Wurtz, R. H. (1998). Response to motion in extrastriate area MSTl: Center-surround interactions. *Journal of Neurophysiology, 80,* 282–296. [PubMed] [Article]

Fang, F., & He, S. (2004). Strong influence of test patterns on the perception of motion aftereffect and position. *Journal of Vision, 4*(7):9, 637–642, http://journalofvision.org/4/7/9/, doi:10.1167/4.7.9. [PubMed] [Article]

Fize, D., Vanduffel, W., Nelissen, K., Denys, K., Chef d'Hotel, C., Faugeras, O., et al. (2003). The retinotopic organization of primate dorsal V4 and surrounding areas: A functional magnetic resonance imaging study in awake monkeys. *Journal of Neuroscience, 23,* 7395–7406. [PubMed] [Article]

Fredericksen, R. E., Verstraten, F. A., & van de Grind, W. A. (1997). Pitfalls in estimating motion detector receptive field geometry. *Vision Research, 37,* 99–119. [PubMed]

Gardner, J. L., Merriam, E. P., Movshon, J. A., & Heeger, D. J. (2008). Maps of visual space in human occipital cortex are retinotopic, not spatiotopic. *Journal of Neuroscience, 28,* 3988–3999. [PubMed] [Article]

Gattass, R., & Gross, C. G. (1981). Visual topography of striate projection zone (MT) in posterior superior temporal sulcus of the macaque. *Journal Neurophysiology, 46,* 621–638. [PubMed]

Gattass, R., Nascimento-Silva, S., Soares, J. G., Lima, B., Jansen, A. K., Diogo, A. C., et al. (2005). Cortical visual areas in monkeys: Location, topography, connections, columns, plasticity and cortical dynamics. *Philosophical Transactions of the Royal Society of London B: Biological Sciences, 360,* 709–731. [PubMed] [Article]

Geesaman, B. J., Born, R. T., Andersen, R. A., & Tootell, R. B. (1997). Maps of complex motion selectivity in the superior temporal cortex of the alert macaque monkey: A double-label 2-deoxyglucose study. *Cerebral Cortex, 7,* 749–757. [PubMed] [Article]

Grill-Spector, K., & Malach, R. (2004). The human visual cortex. *Annual Review of Neuroscience, 27,* 649–677. [PubMed]

Huk, A. C., Dougherty, R. F., & Heeger, D. J. (2002). Retinotopy and functional subdivision of human areas MT and MST. *Journal of Neuroscience, 22,* 7195–7205. [PubMed] [Article]

Husain, M., & Jackson, S. R. (2001). Vision: Visual space is not what it appears to be. *Current Biology, 11,* R753–R755. [PubMed] [Article]

Jones, H. E., Grieve, K. L., Wang, W., & Sillito, A. M. (2001). Surround suppression in primate V1. *Journal of Neurophysiology, 86,* 2011–2028. [PubMed] [Article]

Lyon, D. C., Xu, X., Casagrande, V. A., Stefansic, J. D., Shima, D., & Kaas, J. H. (2002). Optical imaging reveals retinotopic organization of dorsal V3 in New World owl monkeys. *Proceedings of the National Academy of Sciences of the United States of America, 99,* 15735–15742. [PubMed] [Article]

Mareschal, I., Ashida, H., Bex, P. J., Nishida, S., & Verstraten, F. A. (1997). Linking lower and higher stages of motion processing? *Vision Research, 37,* 1755–1759. [PubMed]

Mather, G., Verstraten, F. A., & Anstis, S. M. (1998). *The motion aftereffect: A modern perspective*. Cambridge, MA: MIT Press.

Maunsell, J. H., & Newsome, W. T. (1987). Visual processing in monkey extrastriate cortex. *Annual Review of Neuroscience, 10,* 363–401. [PubMed]

Maunsell, J. H., & Van Essen, D. C. (1983). Functional properties of neurons in middle temporal visual area of the macaque monkey. II. Binocular interactions and sensitivity to binocular disparity. *Journal of Neurophysiology, 49,* 1148–1167. [PubMed]

Melcher, D. (2005). Spatiotopic transfer of visual-form adaptation across saccadic eye movements. *Current Biology, 15,* 1745–1748. [PubMed] [Article]

Melcher, D., & Morrone, M. C. (2003). Spatiotopic temporal integration of visual motion across saccadic eye movements. *Nature Neuroscience, 6,* 877–881. [PubMed]

Merriam, E. P., & Colby, C. L. (2005). Active vision in parietal and extrastriate cortex. *Neuroscientist, 11,* 484–493. [PubMed]

Merriam, E. P., Genovese, C. R., & Colby, C. L. (2003). Spatial updating in human parietal cortex. *Neuron, 39,* 361–373. [PubMed] [Article]

Merriam, E. P., Genovese, C. R., & Colby, C. L. (2007). Remapping in human visual cortex. *Journal of Neurophysiology, 97,* 1738–1755. [PubMed] [Article]

Nakamura, K., & Colby, C. L. (2002). Updating of the visual representation in monkey striate and extrastriate cortex during saccades. *Proceedings of the National Academy of Sciences of the United States of America, 99,* 4026–4031. [PubMed] [Article]

Nakayama, K., Silverman, G. H., Macleod, D. I., & Mulligan, J. (1985). Sensitivity to shearing and compressive motion in random dots. *Perception, 14,* 225–238. [PubMed]

Palmer, S. E. (1999). *Vision science photons to phenomenology*. Cambridge, MA: MIT Press.

Pelli, D. G. (1997). The VideoToolbox software for visual psychophysics: Transforming numbers into movies. *Spatial Vision, 10,* 437–442. [PubMed]

Pettigrew, J. D., Sanderson, K., & Levick, W. R. (1986). *Visual neuroscience*. Cambridge: Cambridge University Press.

Raiguel, S., Van Hulle, M. M., Xiao, D. K., Marcar, V. L., Lagae, L., & Orban, G. A. (1997). Size and shape of receptive fields in the medial superior temporal area (MST) of the macaque. *Neuroreport, 8,* 2803–2808. [PubMed]

Raiguel, S., Van Hulle, M. M., Xiao, D. K., Marcar, V. L., & Orban, G. A. (1995). Shape and spatial distribution of receptive fields and antagonistic motion surrounds in the middle temporal area (V5) of the macaque. *European Journal of Neuroscience, 7,* 2064–2082. [PubMed]

Reppas, J. B., Niyogi, S., Dale, A. M., Sereno, M. I., & Tootell, R. B. (1997). Representation of motion boundaries in retinotopic human visual cortical areas. *Nature, 388,* 175–179. [PubMed]

Ross, J., Morrone, M. C., Goldberg, M. E., & Burr, D. C. (2001). Changes in visual perception at the time of saccades. *Trends in Neurosciences, 24,* 113–121. [PubMed]

Schatler, W. L., & Zaidi, Q. (1993). Effect of spatial configuration on motion aftereffects. *Journal of the Optical Society of America A, Optics and Image Science, 10,* 1433–1449. [PubMed]

Snowden, R. J., & Milne, A. B. (1996). The effects of adapting to complex motions: Position invariance and tuning to spiral motions. *Journal of Cognitive Neuroscience, 8,* 435–452.

Snowden, R. J., & Milne, A. B. (1997). Phantom motion after effects-evidence of detectors for the analysis of optic flow. *Current Biology, 7,* 717–722. [PubMed] [Article]

Tadin, D., Lappin, J. S., Gilroy, L. A., & Blake, R. (2003). Perceptual consequences of centre-surround antagonism in visual motion processing. *Nature, 424,* 312–315. [PubMed]

Tanaka, K., Hikosaka, K., Saito, H., Yukie, M., Fukada, Y., & Iwai, E. (1986). Analysis of local and wide-field movements in the superior temporal visual areas of the macaque monkey. *Journal of Neuroscience, 6,* 134–144. [PubMed] [Article]

Tolias, A. S., Smirnakis, S. M., Augath, M. A., Trinath, T., & Logothetis, N. K. (2001). Motion processing in the macaque: Revisited with functional magnetic resonance imaging. *Journal of Neuroscience, 21,* 8594–8601. [PubMed] [Article]

Tootell, R. B., Hamilton, S. L., Silverman, M. S., & Switkes, E. (1988). Functional anatomy of macaque striate cortex. I. Ocular dominance, binocular interactions, and baseline conditions. *Journal of Neuroscience, 8,* 1500–1530. [PubMed] [Article]

Tootell, R. B., Reppas, J. B., Kwong, K. K., Malach, R., Born, R. T., Brady, T. J., et al. (1995). Functional-analysis of human MT and related visual cortical areas using magnetic resonance imaging. *Journal of Neuroscience, 15,* 3215–3230. [PubMed] [Article]

Tootell, R. B., Silverman, M. S., Hamilton, S. L., De Valois, R. L., & Switkes, E. (1988). Functional anatomy of macaque striate cortex: III. Color. *Journal of Neuroscience, 8,* 1569–1593. [PubMed] [Article]

Tootell, R. B., Switkes, E., Silverman, M. S., & Hamilton, S. L. (1988). Functional anatomy of macaque striate cortex. II. Retinotopic organization. *Journal of Neuroscience, 8,* 1531–1568. [PubMed] [Article]

van Doorn, A. J., & Koenderink, J. J. (1982). Spatial properties of the visual detectability of moving spatial white noise. *Experimental Brain Research, 45,* 189–195. [PubMed]

Van Essen, D. C., Maunsell, J. H., & Bixby, J. L. (1981). The middle temporal visual area in the macaque: Myeloarchitecture, connections, functional properties and topographic organization. *Journal of Comparative Neurology, 199,* 293–326. [PubMed]

Verstraten, F. A. (1996). On the ancient history of the direction of the motion aftereffect. *Perception, 25,* 1177–1187. [PubMed]

von Grünau, M., & Dubé, S. (1992). Comparing local and remote motion aftereffects. *Spatial Vision, 6,* 303–314. [PubMed]

von Grünau, M. W. (1986). A motion aftereffect for long-range stroboscopic apparent motion. *Perception & Psychophysics, 40,* 31–38. [PubMed]

Wade, N. J., Spillmann, L., & Swanston, M. T. (1996). Visual motion aftereffects: Critical adaptation and test conditions. *Vision Research, 36,* 2167–2175. [PubMed]

Weisstein, N., Harris, C. S., Berbaum, K., Tangney, J., & Williams, A. (1977). Contrast reduction by small localized stimuli: Extensive spatial spread of above-threshold orientation-selective masking. *Vision Research, 17,* 341–350. [PubMed]

Werner, J. S., & Chalupa, L. M. (2004). *The visual neurosciences*. Cambridge, MA: MIT Press.

Xiao, D. K., Raiguel, S., Marcar, V., Koenderink, J., & Orban, G. A. (1995). Spatial heterogeneity of inhibitory surrounds in the middle temporal visual area. *Proceedings of the National Academy of Sciences of the United States of America, 92,* 11303–11306. [PubMed] [Article]

Xiao, D. K., Raiguel, S., Marcar, V., & Orban, G. A. (1997). The spatial distribution of the antagonistic surround of MT/V5 neurons. *Cerebral Cortex, 7,* 662–677. [PubMed] [Article]